High-spin states and collective oblate bands in the odd-odd ^{138}Pr nucleus

M. L. Li,[1] S. J. Zhu,[1,*] X. L. Che,[1] Y. N. Yu,[1] Y. J. Chen,[1] H. B. Ding,[1] L. H. Zhu,[2] X. G. Wu,[2] S. X. Wen,[2] C. Y. He,[2] X. Z. Cui,[2] and Y. Liu[2]

[1]*Department of Physics, Tsinghua University, Beijing 100084, People's Republic of China*

[2]*China Institute of Atomic Energy, Beijing, 102413, People's Republic of China*

(Received 6 July 2006; revised manuscript received 21 December 2006; published 14 March 2007)

High-spin states in the odd-odd ^{138}Pr nucleus were reinvestigated with the reaction ^{128}Te(^{14}N, 4n) at a beam energy of 64 MeV. Six collective bands were observed, and two of them were newly identified. For the $\pi h_{11/2} \otimes \nu h_{11/2}$ band, high-spin states are followed up to $I^{\pi} = 16^{+}$. The spin values for this band have been reassigned based on the systematical comparison with the neighboring nuclei. The observed band crossing is proposed to be due to the alignment of protons, and the signature inversion with the neutron number changing in La and Pr isotopes has been discussed. The other five collective bands are proposed to be based on oblate deformation with $\gamma \sim -60^{\circ}$.

DOI: 10.1103/PhysRevC.75.034304 PACS number(s): 23.20.Lv, 21.10.Re, 27.60.+j, 25.85.Ca

I. INTRODUCTION

The odd-odd ^{138}Pr nucleus with $Z = 59$ and $N = 79$ lies in the transitional region with the neutron number approaching the closed shell at $N = 82$. In this region, the nuclei have a small quadrupole deformation parameter β_2 and a soft γ deformation. The proton Fermi surface lies in the lower $h_{11/2}$ subshell, whereas the neutron Fermi surface lies in the upper $h_{11/2}$ subshell. The rotational alignment of a pair of $h_{11/2}$ protons tends to drive the nucleus to a near prolate ($\gamma \sim 0^{\circ}$) shape, whereas the rotational alignment of a pair of $h_{11/2}$ neutrons tends to drive the nucleus to a near oblate ($\gamma \sim -60^{\circ}$) shape (Lund convention [1]). Therefore, the different quasiparticle configurations can drive a nucleus to different shapes and sometimes shape coexistence may be observed in a nucleus [2]. In the previous publications, one of the important structures in this region is the observation of collective oblate bands. The first oblate band based on $\pi h_{11/2} \otimes (\nu h_{11/2})^2$ configuration was found in ^{131}La by E. S. Paul *et al*. [3]. To date oblate bands, for example, in ^{132,133}Ba [4,5], $^{134-137}$La [6–9], ^{135,137,138}Ce [10–12], ^{137}Pr [13], and ^{139}Pm [14], have been reported. However, systematical signature inversion in odd-odd nuclei is also an interesting subject [15,16], and this phenomenon is still not fully understood theoretically.

It is expected that at the low-spin states the ^{138}Pr nucleus should have stronger noncollectivity than the $N < 79$ neighboring Pr isotopes as its neutron number is closer to the closed shell at $N = 82$. In the previous works, for the odd-odd Pr isotopes, the high-spin structures in ^{134}Pr [17] and ^{136}Pr [18] have been studied in detail. For the ^{138}Pr nucleus, the low-spin states have been studied from the β decay [19], and some high-spin levels and band structures were reported using a heavy-ion reaction [20], but one still needs to extend its high-spin states to systematically understand the nuclear structure character of the double-odd nuclei in this region, such as the signature inversion, the band crossing, the oblate bands etc.. In this article, we report on experimental research on high-spin states and collective-band structures in ^{138}Pr in more detail. When this work was in progress, Gangopadhyay *et al*. [21] published some high-spin states in ^{138}Pr. Comparing with the results obtained in Ref. [21], we significantly updated the high-spin scheme of ^{138}Pr, and many new levels and transitions have been identified.

II. EXPERIMENTS AND RESULTS

High-spin states in ^{138}Pr were populated via the ^{128}Te(^{14}N, 4n) fusion-evaporation reaction at a beam energy of 64 MeV. An isotopically enriched ^{128}Te target of thickness 3.3 mg/cm^2 was bombarded by the beam of ^{14}N ions accelerated by the HI-13 tandem accelerator at the China Institute of Atomic Energy (CIAE). The γ-γ coincidence measurement was carried out using an array of 14 Compton-suppressed Ge detectors. The energy resolutions of the Ge detectors are between 1.8 and 2.2 keV at 1.333 MeV γ-ray energy. Approximately 2.3×10^8 coincidence events were collected, from which a γ-γ coincidence matrix was built. The relative efficiencies were calibrated using a ^{152}Eu source. To determine the multipolarity of the γ-ray transitions the five detectors near 90°, with respect to the beam axis, were sorted against the other nine detectors at 45° (three), 55° (one), 125° (one), and 135° (four) to produce a two-dimensional angular-correlation matrix, from which it was possible to extract the average directional correlation of oriented state (DCO) intensity ratios. The γ-γ coincidence data were analyzed with the Radware software package [22].

The level scheme of ^{138}Pr deduced from the present work is shown in Fig. 1. It was based on the γ-γ coincidence relationships, the relative transition intensities and the DCO ratio analysis. Collective bands observed are labeled on the top of the scheme. Some of the coincidence γ-ray spectra are shown in Figs. 2 and 3. In Fig. 2(a) a coincidence spectrum is obtained by gating on the 136.0 keV [$(10^+) \rightarrow (9^+)$ in band (1)] transition, where the transitions in bands (1), (2), and (4) can be seen. Figure 2(b) shows a spectrum obtained

*Electronic address: zhushj@mail.tsinghua.edu.cn

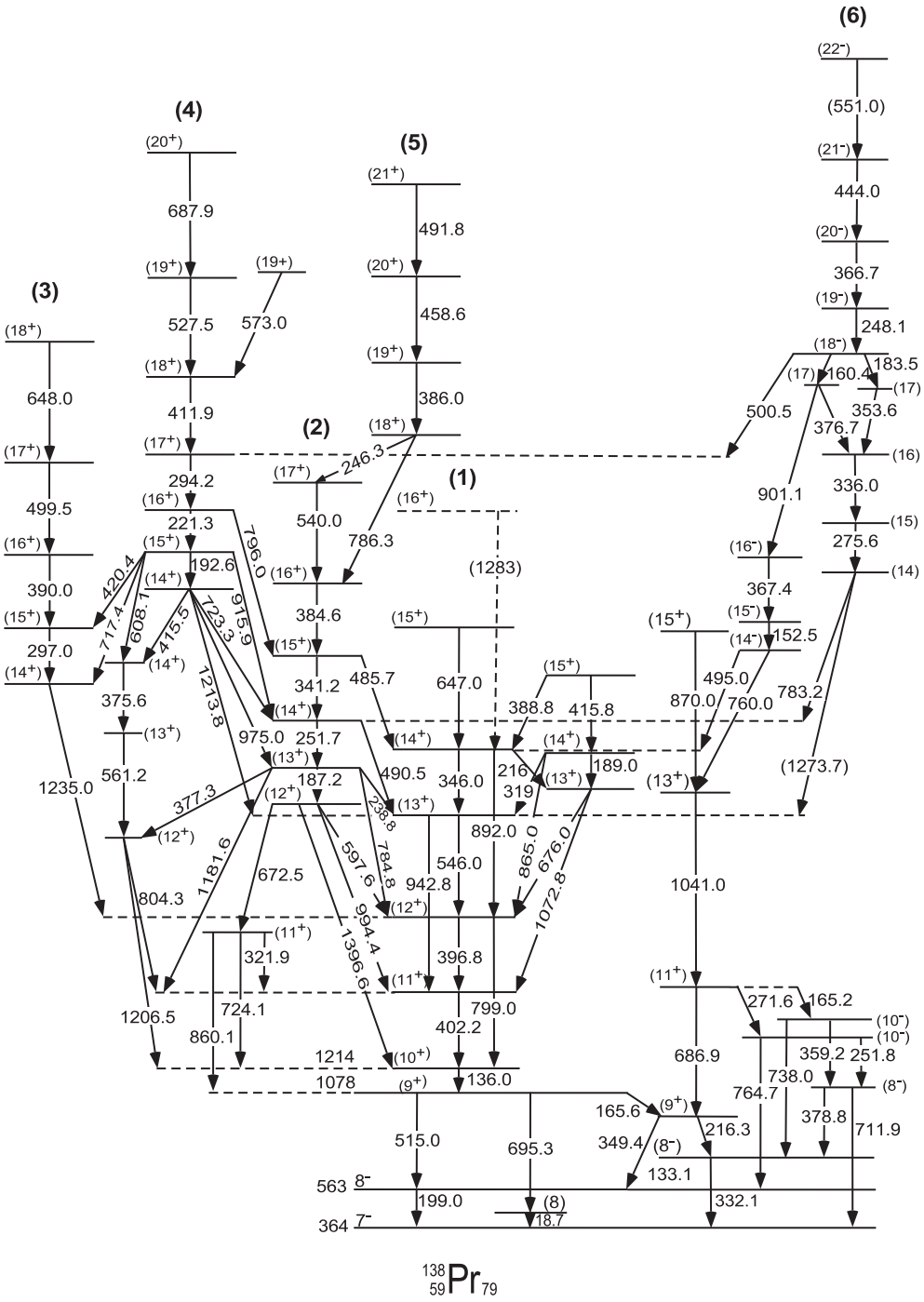

FIG. 1. Proposed level scheme of ^{138}Pr. The transition energies are given in keV.

by gating on the 1235.0-keV [$(14^+) \rightarrow (12^+)$ from band (3) to band (1)] transition, and some transitions in band (3) can be seen. In Fig. 2(c), a coincidence spectrum is generated by gating on the 386.0-keV [$(19^+) \rightarrow (18^+)$ in band (5)] transition. From this spectrum, the transitions in bands (2) and (5) can be seen. Figs. 3(a) and 3(b) show the coincidence transitions relative to the right-side states in Fig. 1 by gating on the 271.6 [$(11^+) \rightarrow (10^-)$ at the low-spin states of the right side in Fig. 1] and 248.1-keV [$(19^-) \rightarrow (18^-)$ in band (6)] transitions, respectively. In all spectra, one can also see the corresponding coincident γ peaks at the lower-spin states.

Most of the levels and transitions observed in Refs. [20,21] were confirmed in the present work. Moreover, we add 14 new levels and 25 new γ transitions to the scheme, comparing our results to those reported in Ref. [21]. Two new bands (3) and (5) were newly identified in the present work. Some collective band structures reported in Ref. [21] were updated.

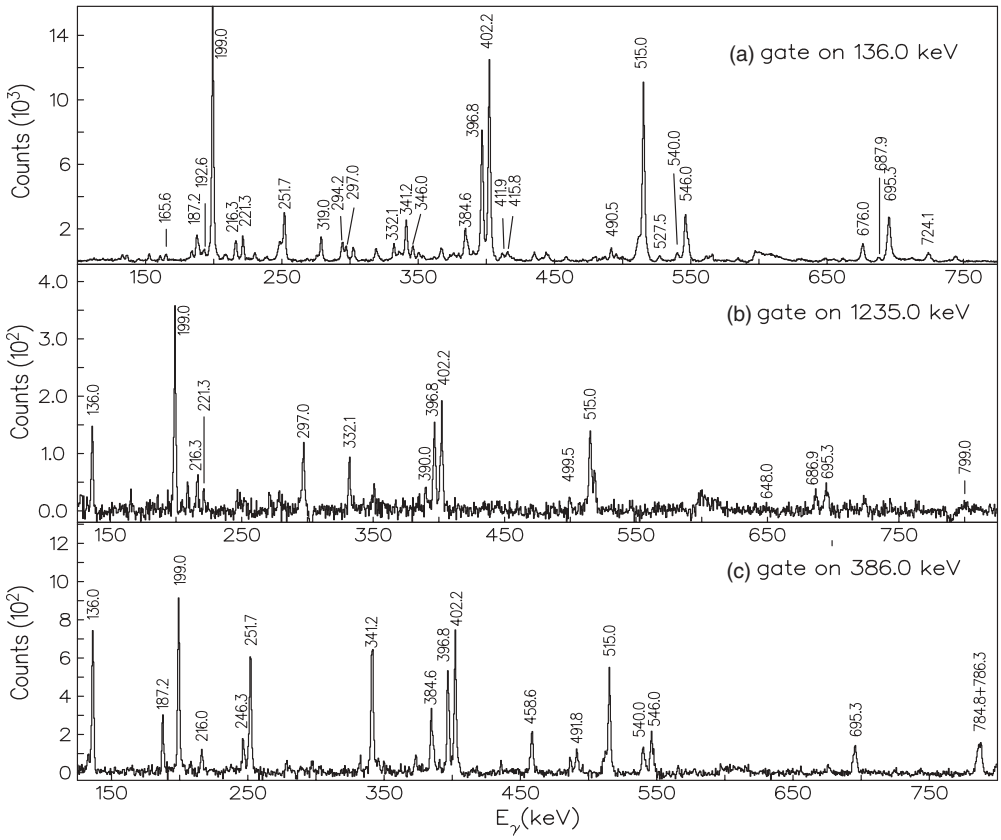

FIG. 2. Coincidence spectra by gating on (a) 136.0-keV, (b) 1235.0-keV, and (c) 386.0-keV γ transitions.

III. DISCUSSION

The spin and parity (I^π) assignments for some levels are based on the previous works [19–21], the DCO ratios, and the systematical comparison with the levels of neighboring $N = 79$ isotones ^{136}La [8] and ^{140}Pm [23]. Table I shows the observed DCO ratios for some γ-transitions of ^{138}Pr in the present work. The DCO ratios for some weak transitions could not be obtained because of the poor statistics of the γ peaks. Generally, a quadrupole ($\Delta I = 2$, $E2$) transition is adopted if a DCO ratio is around 1.35, and a dipole ($\Delta I = 1$) transition is assumed if a DCO ratio is around 0.85. Most of the transitions belong to dipole transitions in the present level scheme and only six DCO ratios of the quadrupole transitions, 686.9, 786.3, 799.0, 870.0, 1041.0, and 1235.0 keV were obtained. The ground state of ^{138}Pr is built on an 1^+ state with a half-life of 0.4 min [19]. The lowest state in Fig. 1 is a first isomeric state ($T_{1/2} = 2.12$ h) at 364 keV with $I^\pi = 7^-$ [19–21] and the I^π of 563-keV level is assigned as 8^-, which is consistent with that in Ref. [21]. However, above the 563-keV level, we reassign the I^π's of the levels in band (1). Generally, it is rather difficult to assign the I^π of the band in odd-odd A nuclei. A key step is to determine the I^π of the band head level, i.e., the 1078-keV level in ^{138}Pr. This level was tentatively assigned as 8^+ state in Ref. [20] and was determined as the same state according to the DCO ratios in Ref. [21]. The linking 515-keV γ transition from the 1078-keV level to the 563-keV level belongs to a dipole transition [21] that is confirmed by the present work. However, in a dipole transition, one cannot distinguish between $E1$ and $M1/E2$ transitions or between $\Delta I = 0$ and $\Delta I = 1$ transitions using this method. So the I^π of the band head level in band (1) is still undetermined only using the DCO ratio. The band (1) is built on $\pi h_{11/2} \otimes \nu h_{11/2}$ configuration [20,21]. A practical method to determine the spin values of this band is based on the assumption that the excitation energy with the same spin in a chain of deformed odd-odd isotopes and isotones varies in a smooth way [15,24–26]. Using this method, for many odd-odd nuclei in this region, the spin values of the $\pi h_{11/2} \otimes \nu h_{11/2}$ bands have been reassigned, including those in ^{130,132,134,136}Pr [15]. So we reassigned the spins of the band (1) of ^{138}Pr according to this method also. For the yrast $\pi h_{11/2} \otimes \nu h_{11/2}$ configuration the "favored" $\alpha = 1$ signature was defined as odd-spin levels, whereas the "unfavored" $\alpha = 0$ signature was defined as even-spin levels. Figures 4(a) and 4(b) show excitation energy systematics of $\alpha = 1$ and $\alpha = 0$ sequences of the $\pi h_{11/2} \otimes \nu h_{11/2}$ bands in odd-odd nuclei $^{130-138}$Pr, respectively, and the level schemes of $\pi h_{11/2} \otimes \nu h_{11/2}$ bands in the isotonic chain with $N = 79$ are shown in Fig. 5. One can see when the spin value of the band head level at 1078 keV in the band (1) of ^{138}Pr is taken as $9\hbar$ instead of $8\hbar$ adopted in Ref. [21], the positions of the levels with the same spin fit to the smooth variation very well. Based on this systematic comparison, we assigned the I^π of the band head level at 1078 keV of the band (1) as 9^+ instead of 8^+ assigned in Ref. [21]. So the spin values of the other levels in band (1) should be added with one $\hbar$ comparing with

TABLE I. Measured DCO ratios of some γ transitions in ^{138}Pr.

E_γ(keV)	$R_{\rm DCO}$	Assignment	Mult.	Bands
136.0	0.91(4)	$(10^+) \rightarrow (9^+)$	$M1/E2$	(1)
160.4	1.02(41)	$(18^-) \rightarrow (17)$	$(M1/E2, E1)$	(6) $\rightarrow$ under (6)
183.5	1.05(35)	$(18^-) \rightarrow (17)$	$(M1/E2, E1)$	(6) $\rightarrow$ under (6)
187.2	0.98(11)	$(13^+) \rightarrow (12^+)$	$M1/E2$	(2)
192.6	1.03(15)	$(15^+) \rightarrow (14^+)$	$M1/E2$	(4)
199.0	0.74(2)	$8^- \rightarrow 7^-$	$M1/E2$	Under (1)
221.3	0.79(14)	$(16^+) \rightarrow (15^+)$	$M1/E2$	(4)
251.7	0.90(7)	$(14^+) \rightarrow (13^+)$	$M1/E2$	(2)
297.0	0.80(12)	$(15^+) \rightarrow (14^+)$	$M1/E2$	(3)
332.1	0.89(4)	$(8^-) \rightarrow 7^-$	$M1/E2$	Under (6)
341.2	0.99(10)	$(15^+) \rightarrow (14^+)$	$M1/E2$	(2)
346.0	1.01(17)	$(14^+) \rightarrow (13^+)$	$M1/E2$	(1)
349.4	0.81(9)	$(9^+) \rightarrow 8^-$	$(E1)$	Under (6)
353.6	1.01(25)	$(17) \rightarrow (16)$	$(M1/E2, E1)$	Under (6)
366.7	0.98(23)	$(20^-) \rightarrow (19^-)$	$M1/E2$	(6)
396.8	0.91(4)	$(12^+) \rightarrow (11^+)$	$M1/E2$	(1)
402.2	0.80(3)	$(11^+) \rightarrow (10^+)$	$M1/E2$	(1)
411.9	0.85(21)	$(18^+) \rightarrow (17^+)$	$M1/E2$	(4)
444.0	0.86(34)	$(21^-) \rightarrow (20^-)$	$M1/E2$	(6)
515.0	0.68(2)	$(9^+) \rightarrow 8^-$	$(E1)$	Under (1)
527.5	0.62(21)	$(19^+) \rightarrow (18^+)$	$M1/E2$	(4)
540.0	0.78(20)	$(17^+) \rightarrow (16^+)$	$M1/E2$	(2)
546.0	0.57(4)	$(13^+) \rightarrow (12^+)$	$M1/E2$	(1)
676.0	0.72(8)	$(13^+) \rightarrow (12^+)$	$(M1/E2)$	Side (1) $\rightarrow$ (1)
686.9	1.15(12)	$(11^+) \rightarrow (9^+)$	$E2$	Under (6)
695.3	0.71(3)	$(9^+) \rightarrow (8)$	$(M1/E2, E1)$	(1) $\rightarrow$ under (1)
784.8	0.78(9)	$(13^+) \rightarrow (12^+)$	$(M1/E2)$	(2) $\rightarrow$ (1)
786.3	1.46(34)	$(18^+) \rightarrow (16^+)$	$E2$	(5) $\rightarrow$ (2)
799.0	1.43(18)	$(12^+) \rightarrow (10^+)$	$E2$	(1)
870.0	1.09(32)	$(15^+) \rightarrow (13^+)$	$E2$	Under (6)
1041.0	1.52(17)	$(13^+) \rightarrow (11^+)$	$E2$	Under (6)
1235.0	1.31(33)	$(14^+) \rightarrow (12^+)$	$E2$	(3) $\rightarrow$ (1)

those in Ref. [21]. From the new spin values in the band (1) and the DCO ratios, we assigned the I^π's of the other levels in ^{138}Pr, as shown in Fig. 1.

Now we examine the signature inversion of the $\pi h_{11/2} \otimes \nu h_{11/2}$ bands at low-spin states in this region. The signature inversion means that the expected energetically "unfavored" signature component of certain bands actually lies lower in energy than the corresponding "favored" component (e.g., see Ref. [27] and references therein). The plots of $[E(I)\text{-}E(I\text{-}1)]/2I$ versus I for the $\pi h_{11/2} \otimes \nu h_{11/2}$ bands of ^{130,132,134,136}Pr [15,17,18,28] (the spins were reassigned in Ref. [15] and then the levels were expanded in Refs. [17,18,28]), ^{138}Pr (present work), ^{132}La [29], ^{134}La [30], and ^{136}La [8] are shown in Fig. 6. The solid dots correspond to favored signature ($\alpha = 1$, odd spin), whereas the open circles correspond to unfavored signature ($\alpha = 0$, even spin). Some systematic features can be seen from Fig. 6. First, the low-spin signature of the $\pi h_{11/2} \otimes \nu h_{11/2}$ band is inverted for all these nuclei, including in ^{138}Pr. This is what happened in the $\pi h_{11/2} \otimes \nu h_{11/2}$ bands of other double-odd nuclei around $A \sim 130$ [15]. The signature inversion in low-spin states in ^{138}Pr is consistent with the systematics. Second, inversion spin $I_{\rm inv}$ (indicated by arrows in Fig. 6) decreases with increasing neutron number from ^{132}La to ^{136}La where the inversion point has been observed. In contrast, the inversion spin $I_{\rm inv}$ increases with increasing neutron number in the $N < 73$ La isotopes [15]. So, the inversion spin $I_{\rm inv}$ firstly increases and then decreases with increasing neutron number for La isotopes. Although the inversion point of several Pr isotopes has not been observed, the inversion spin $I_{\rm inv}$ seems to firstly increase and then decrease with increasing neutron number, too.

Figure 7 shows the aligned momenta i_x of band (1) against the rotational frequency $\hbar\omega$. The reference configuration was taken from the Harris parametrization of the moment of inertia [31] $J_0 = 19.7$ MeV$^{-1}\hbar^2$ and $J_1 = 50.9$ MeV$^{-3}\hbar^4$, extracted by fitting the yrast band members below the backbend in the ^{136}Ce nucleus. One can see that a band crossing (backbending) occurs at $\hbar\omega \sim 0.36$ MeV. To understand the band crossing property observed in ^{138}Pr, we have carried out the cranked shell-model (CSM) calculations described in detail by Bengtsson *et al.* [32] and Frauendorf *et al.* [33,34]. The parameters used in the calculations were as follows: $\beta_2 = 0.115$, $\beta_4 = -0.016$, $\gamma = 5^\circ$. These parameters were obtained from the minima of our total Rothian surface (TRS)

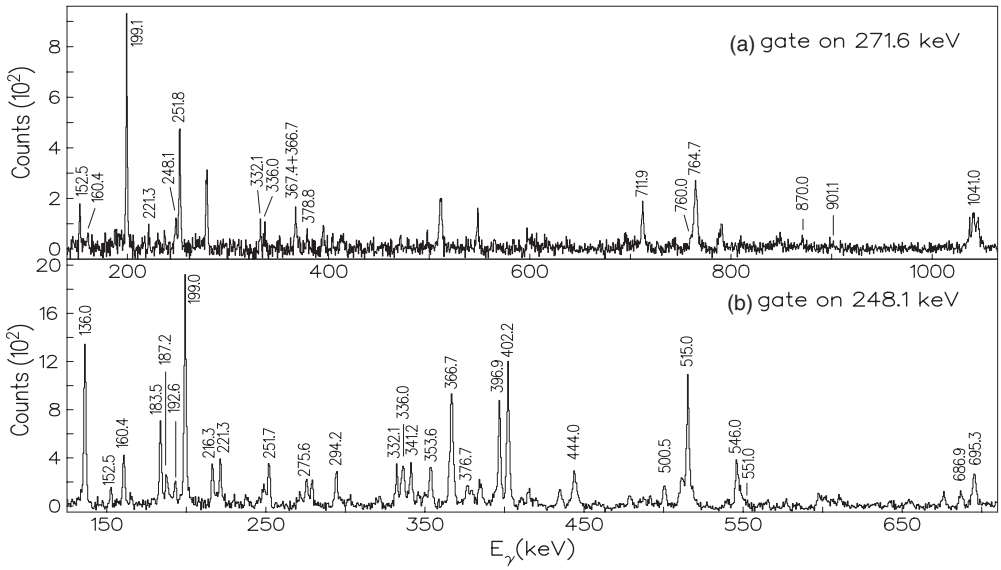

FIG. 3. Coincidence spectra by gating on (a) 271.6-keV and (b) 248.1-keV γ transitions.

calculations. The other parameters were taken as standard. The calculated quasiparticle energies (Routhians) for ^{138}Pr are presented in Fig. 8(a) for protons and in Fig. 8(b) for neutrons, respectively. The Nilsson configurations of the lowest orbitals in Figs. 8(a) and 8(b) are 1/2[550] and 11/2[505], respectively. The calculations predict that a band crossing caused by the alignment of two $h_{11/2}$ protons occurs at $\hbar\omega \sim 0.36$ MeV, which is consistent with the experimental value of $\hbar\omega \sim 0.36$ MeV. So we proposed that the observed band crossing of band (1) in ^{138}Pr probably originates from alignment of $h_{11/2}$ protons. In the neighboring nuclei such as ^{134}Pr [17] and ^{136}Pr [18], the observed band crossing is also due to alignment of protons.

The most interesting finding of the present study is the collective bands (2)–(6). The five bands show similar features to the other known oblate bands in the $A \sim 130$ region: (a) much stronger $\Delta I = 1$ transitions relative to the $\Delta I = 2$ transitions inside the band, (b) no signature splitting occuring, and (c) different moments of inertial ($J^{(1)}$ and $J^{(2)}$) from those of prolate bands. Plots of the moments of inertia $J^{(1)}$ and $J^{(2)}$ of the collective bands (2)–(6) in ^{138}Pr along with the oblate bands in ^{135}La [7], ^{136}La [8], ^{137}Ce [11], and ^{138}Ce [12], as

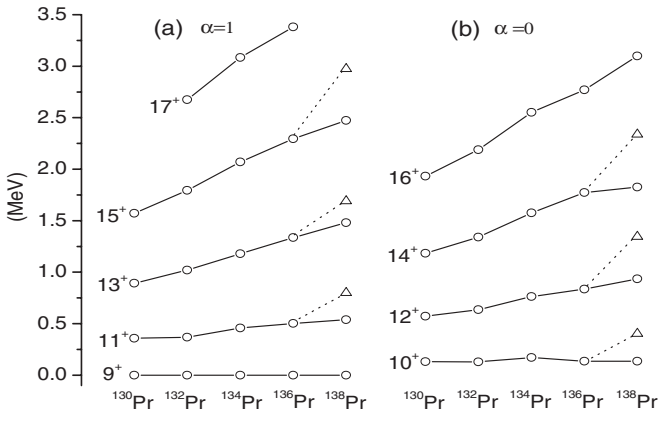

FIG. 4. Excitation energy systematics of (a) $\alpha = 1$ and (b) $\alpha = 0$ sequences of $\pi h_{11/2} \otimes \nu h_{11/2}$ bands in $^{130-138}$Pr. Energies indicating level positions are in MeV. ○ represents the level positions based on present spin assignments, and △ represents the level positions based on previous spin assignments for ^{138}Pr in Ref. [21]. Data sources: ^{130,132,134,136}Pr [15] and ^{138}Pr (present work). The excitation energies are normalized to the 9^+.

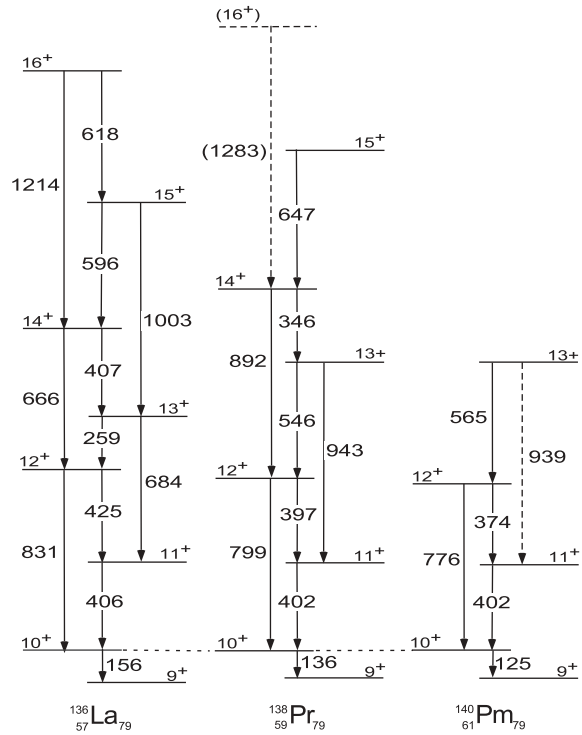

FIG. 5. The level systematics of $\pi h_{11/2} \otimes \nu h_{11/2}$ bands in ^{138}Pr, ^{136}La, and ^{140}Pm. The states with $I = 10\hbar$ are taken as reference for comparison. Energies are given in keV. Data sources: ^{136}La [8], ^{138}Pr (present work), and ^{140}Pm [23].

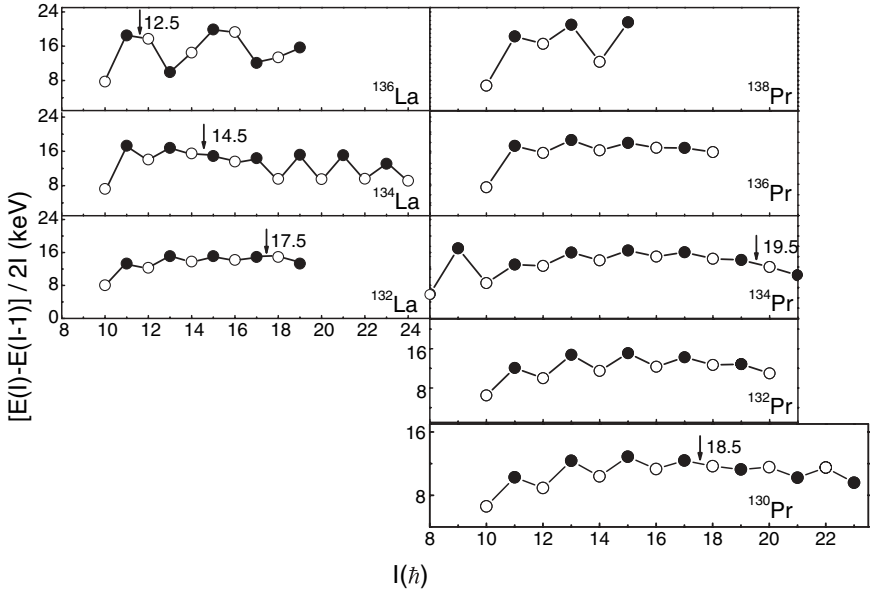

FIG. 6. $[E(I)\text{-}E(I\text{-}1)]/2I$ versus I for the $\pi h_{11/2} \otimes \nu h_{11/2}$ bands in ^{132,134,136}La and ^{130,132,134,136,138}Pr.

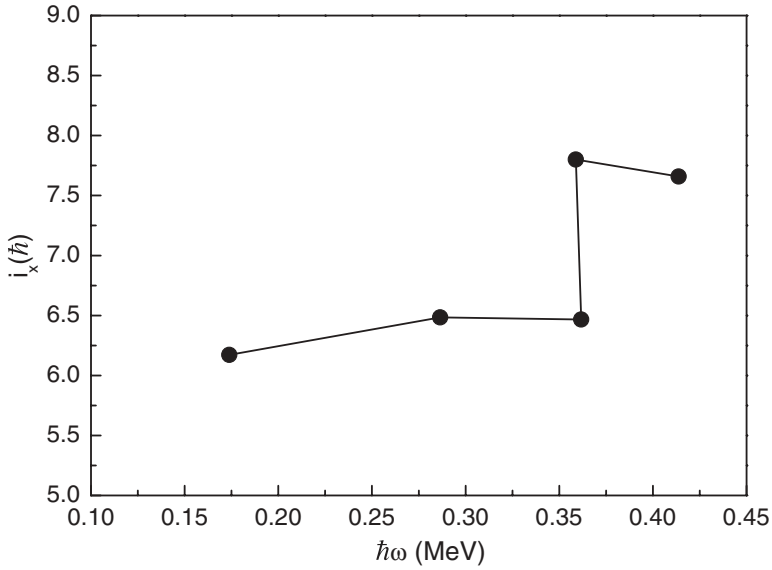

FIG. 7. Experimental alignments of band (1) in ^{138}Pr against the rotational frequency $\hbar\omega$.

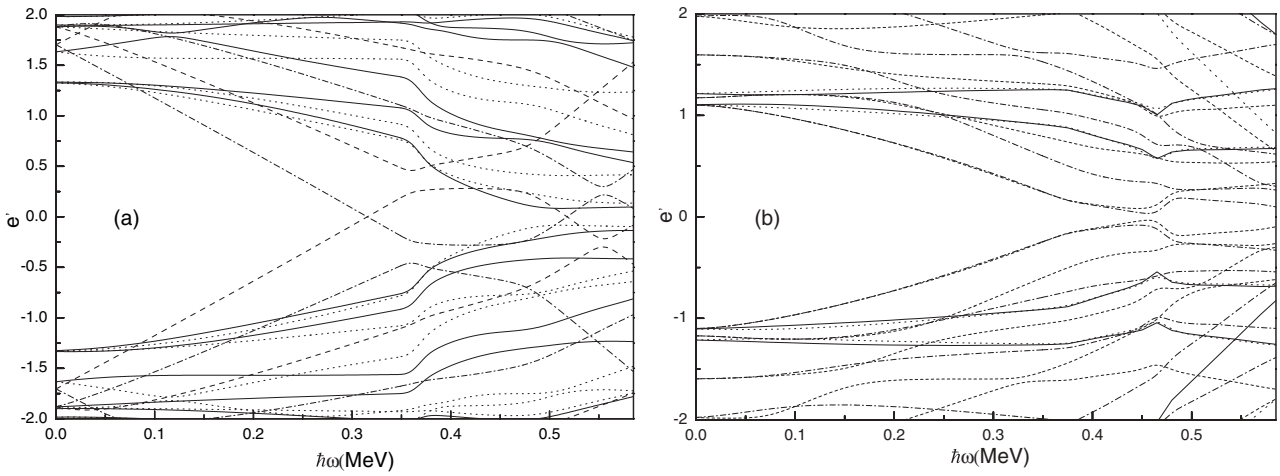

FIG. 8. Plots of the calculated Routhians for quasiprotons (a) and quasineutrons (b) against the rotational frequency $\hbar\omega$. The parity and signature (π, α) of the levels are $(+, +1/2)$ solid lines; $(+, -1/2)$ dotted lines; $(-, +1/2)$ dot-dashed lines; $(-, -1/2)$ dashed lines.

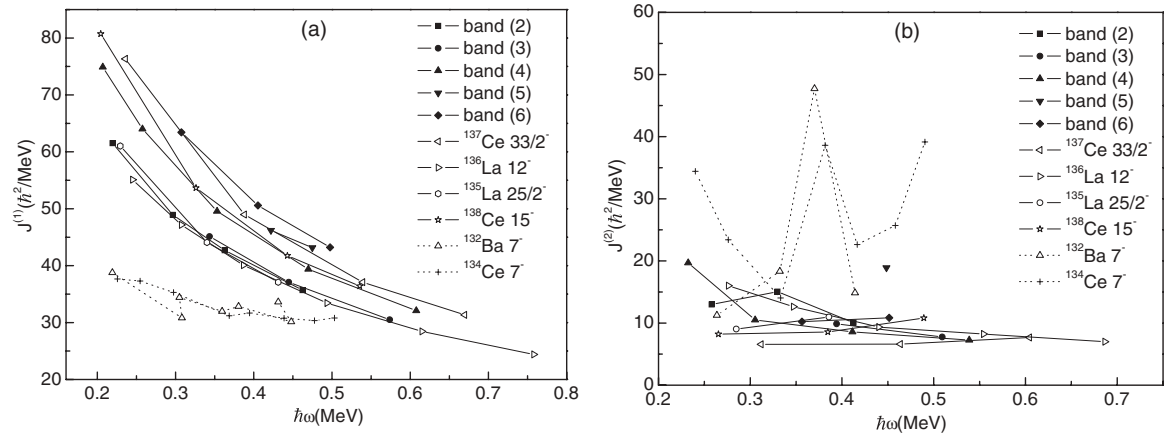

FIG. 9. Comparison of the moments of inertia $J^{(1)}$ (a) and $J^{(2)}$ (b) of bands (2)–(6) in ^{138}Pr with the oblate bands in ^{135}La, ^{136}La, ^{137}Ce, and ^{138}Ce, as well as prolate bands in ^{132}Ba and ^{134}Ce (spin and parity of the band head is labeled).

well as the prolate bands in ^{132}Ba [2] and ^{134}Ce [35], against the rotational frequency $\hbar\omega$ are shown in Fig. 9. One can see that the $J^{(1)}$ and $J^{(2)}$ of the bands (2)–(6) in ^{138}Pr show similar behavior to the oblate bands in the neighboring nuclei but are different from the prolate bands. Some cranked shell-model calculations have been carried out to understand the different shape driving effects of protons and neutrons in this region [2,3]. It shows that the alignment of a pair of $h_{11/2}$ protons favors a prolate shape ($\gamma \sim 0^\circ$) and the alignment of a pair of $h_{11/2}$ neutrons favors an oblate shape ($\gamma \sim -60^\circ$). The proton orbitals close to the Fermi level in this region are $g_{7/2}, d_{5/2}$, and $h_{11/2}$. The neutron orbitals close to the Fermi level are $d_{3/2}$ and $h_{11/2}$. Bands (2), (3), and (4) are probably based on four-quasiparticle configurations and their possible configurations can be assigned as $\pi g_{7/2} \otimes \nu d_{3/2}(h_{11/2})^2$, $\pi d_{5/2} \otimes \nu d_{3/2}(h_{11/2})^2$, $\pi h_{11/2} \otimes \nu(h_{11/2})^3$, respectively. Bands (5) and (6) may belong to six-quasiparticle bands, as the band head energy for these bands is much higher than those in the bands (2), (3), and (4). Possible configurations for bands (5) and (6) may be assigned as $\pi g_{7/2}(d_{5/2})^2 \otimes \nu d_{3/2}(h_{11/2})^2$ and $\pi d_{5/2} g_{7/2} h_{11/2} \otimes \nu d_{3/2}(h_{11/2})^2$, respectively. In each oblate band configuration proposed, a pair of $h_{11/2}$ neutrons is included. It should drive the nucleus to oblate shape with ($\gamma \sim -60^\circ$) at the high-spin states. To accurately assign the configurations needs further study.

IV. CONCLUSION

The high-spin structure of the ^{138}Pr nucleus was studied. Six collective bands were observed. Among them, two bands were newly identified. Many levels and transitions were newly observed. Based on systematical comparison with the neighboring nuclei, the spins of the $\pi h_{11/2} \otimes \nu h_{11/2}$ band were newly assigned. The signature spitting and inversion are systematically discussed. A band crossing, due to the alignment of protons, was observed. The other five bands in ^{138}Pr were proposed to be oblate bands. It may be the first time that the five oblate bands were observed in a nucleus.

ACKNOWLEDGMENTS

The work at Tsinghua University was supported by the National Natural Science Foundation of China under grants 10575057 and 10375032 and the Special Program of High Education Science Foundation under grant 20030003090. The authors thank the staff of the in-beam γ-ray group and their hospitality during the experiment and for providing the heavy-ion beam and the target.

[1] G. Andersson *et al.*, Nucl. Phys. **A268**, 205 (1976).
[2] E. S. Paul, D. B. Fossan, Y. Liang, R. Ma, and N. Xu, Phys. Rev. C **40**, 1255 (1989).
[3] E. S. Paul *et al.*, Phys. Rev. Lett. **58**, 984 (1987).
[4] S. Juutinen, S. Tormanen, P. Ahonen *et al.*, Phys. Rev. C **52**, 2946 (1995).
[5] S. Juutinen, P. Simecek, P. Ahonen *et al.*, Phys. Rev. C **51**, 1699 (1995).
[6] U. Datta Pramanik, A. Mukherjee, P. Basu *et al.*, Nucl. Phys. **A637**, 327 (1998).
[7] P. Luo *et al.*, High Energy Phys. Nucl. Phys. **28**, 495 (2004) (in Chinese).
[8] S. J. Zhu *et al.*, Eur. Phys. J. A **24**, 199 (2005).
[9] M. L. Li, S. J. Zhu *et al.*, Eur. Phys. J. A **28**, 1 (2006).
[10] R. Ma, E. S. Paul, D. B. Fossan *et al.*, Phys. Rev. C **41**, 2624 (1990).
[11] S. J. Zhu *et al.*, Phys. Rev. C **62**, 044310 (2000).
[12] S. J. Zhu *et al.*, Chin. Phys. Lett. **16**, 635 (1999).
[13] N. Xu, C. W. Beausang, R. Ma, E. S. Paul, W. F. Piel, D. B. Fossan, and L. Hildingsson, Phys. Rev. C **39**, 1799 (1989).
[14] N. Xu *et al.*, Phys. Rev. C **36**, R1649 (1987).
[15] Y. Z. Liu, J. B. Lu, Y. J. Ma, S. G. Zhou, and H. Zheng, Phys. Rev. C **54**, 719 (1996).
[16] H. J. Chantler *et al.*, Phys. Rev. C **66**, 014311 (2002).
[17] C. M. Petrache, D. Bazzacco, S. Lunardiet *et al.*, Nucl. Phys. **A597**, 106 (1996).

[18] C. M. Petrache, C. A. Ur, D. Bazzacco *et al*., Nucl. Phys. **A603**, 50 (1996).
[19] A. A. Sonzogni, Nucl. Data Sheets **98**, 515 (2005).
[20] M. A. Rizzutto, E. W. Rizzutto, V. R. Vanin *et al*., Z. Phys. A **344**, 221 (1992).
[21] G. Gangopadhyay, S. Bhowal, R. K. Bhowmik *et al*., Eur. Phys. J. A **24**, 173 (2005).
[22] D. C. Radford, Nucl. Instrum. Methods Phys. Res., Sect. A **361**, 297 (1995).
[23] G. D. Angelis, S. Lunardi, D. Bazzacco *et al*., Z. Phys. A **347**, 93 (1993).
[24] D. J. Hartley *et al*., Phys. Rev. C **63**, 041301(R) (2001).
[25] D. J. Hartley *et al*., Phys. Rev. C **64**, 031304(R) (2001).
[26] K. Starosta *et al*., Phys. Rev. C **65**, 044328 (2002).
[27] J. F. Smith, C. J. Chiara, D. B. Fossan, G. J. Lane, J. F. Lewicki, J. M. Sears, and P. Vaska, Phys. Rev. C **58**, 3237 (1998).
[28] C. M. Petrache, S. Brant, D. Bazzacco *et al*., Nucl. Phys. **A635**, 361 (1988).
[29] V. Kumar, P. Das, R. P. Singh *et al*., Eur. Phys. J. A **17**, 153 (2003).
[30] R. A. Bark, A. M. Baxter, A. P. Byrne *et al*., Nucl. Phys. **A691**, 577 (2001).
[31] S. M. Harris, Phys. Rev. **138**, B509 (1965).
[32] B. Bengtsson and S. Frauendorf, Nucl. Phys. **A327**, 139 (2001).
[33] S. Frauendorf, Phys. Lett. **B100**, 219 (1981).
[34] S. Frauendorf and F. R. May, Phys. Lett. **B125**, 245 (1983).
[35] S. J. Zhu *et al*., High Energy Phys. Nucl. Phys. **29**, 130 (2005) (in Chinese).